Simultaneous Detection of ATP and GTP by Covalently Linked Fluorescent Ribonucleopeptide Sensors

Shun Nakano[†], Masatora Fukuda[†], Tomoki Tamura[†], Reiko Sakaguchi[†], Eiji Nakata[†,‡], and Takashi Morii[†,‡,]*

Contribution from [†]Institute of Advanced Energy Kyoto University, and [‡]CREST, JST, Uji, Kyoto 611-0011, Japan

AUTHOR EMAIL ADDRESS: t-morii@iae.kyoto-u.ac.jp

*To whom correspondence should be addressed.

Supporting Information

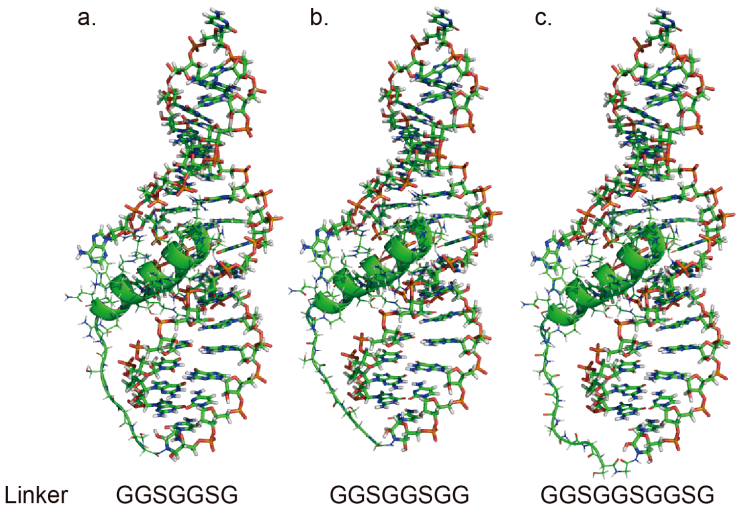

Figure S1. Structural models of the covalently linked Rev-RRE complex. RNA and peptide subunit are linked through a peptide linker (a) GGSGGSG, (b) GGSGGSGG and (c) GGSGGSGGSG. The models were constructed based on the three dimensional structure of Rev-RRE (PDB ID: 1etf)[S1]. The structure of the linker portion was optimized with CHARMm force field by using Discovery Studio ver. 3.1.

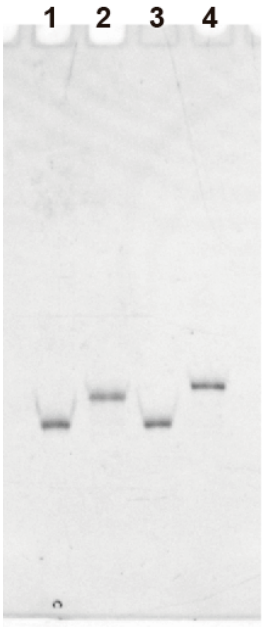

Figure S2. A PAGE image shows purity of the covalently linked RNP sensors. The purity of each sample was confirmed by the denaturing gel electrophoresis (6 M Urea, 15% PAGE). Each lane shows G23 RNA (Lane 1), c-G23/Pyr-Rev (Lane 2), A26 RNA (Lane 3), c-A26/5FAM-Rev (Lane 4), respectively.

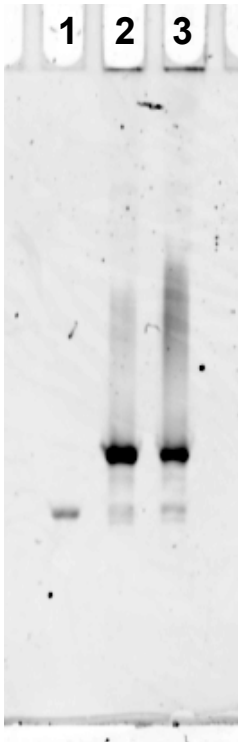

Figure S3. A PAGE image shows formation of the covalently linked A26/5FAM-Rev. The reaction mixture was analyzed by the denaturing gel electrophoresis (6 M Urea, 15% PAGE) and the yield of reaction was calculated from the band intensity by using the Image J software. Each lane shows A26 RNA (Lane 1), c-A26/5FAM-Rev that was formed under the native condition (Lane 2), c-A26/5FAM-Rev that was formed under the denaturing condition containing 6 M Urea (Lane 3), respectively. The ratio of the band corresponding to cRNP was 92% (lane 2) and 89% (lane 3).

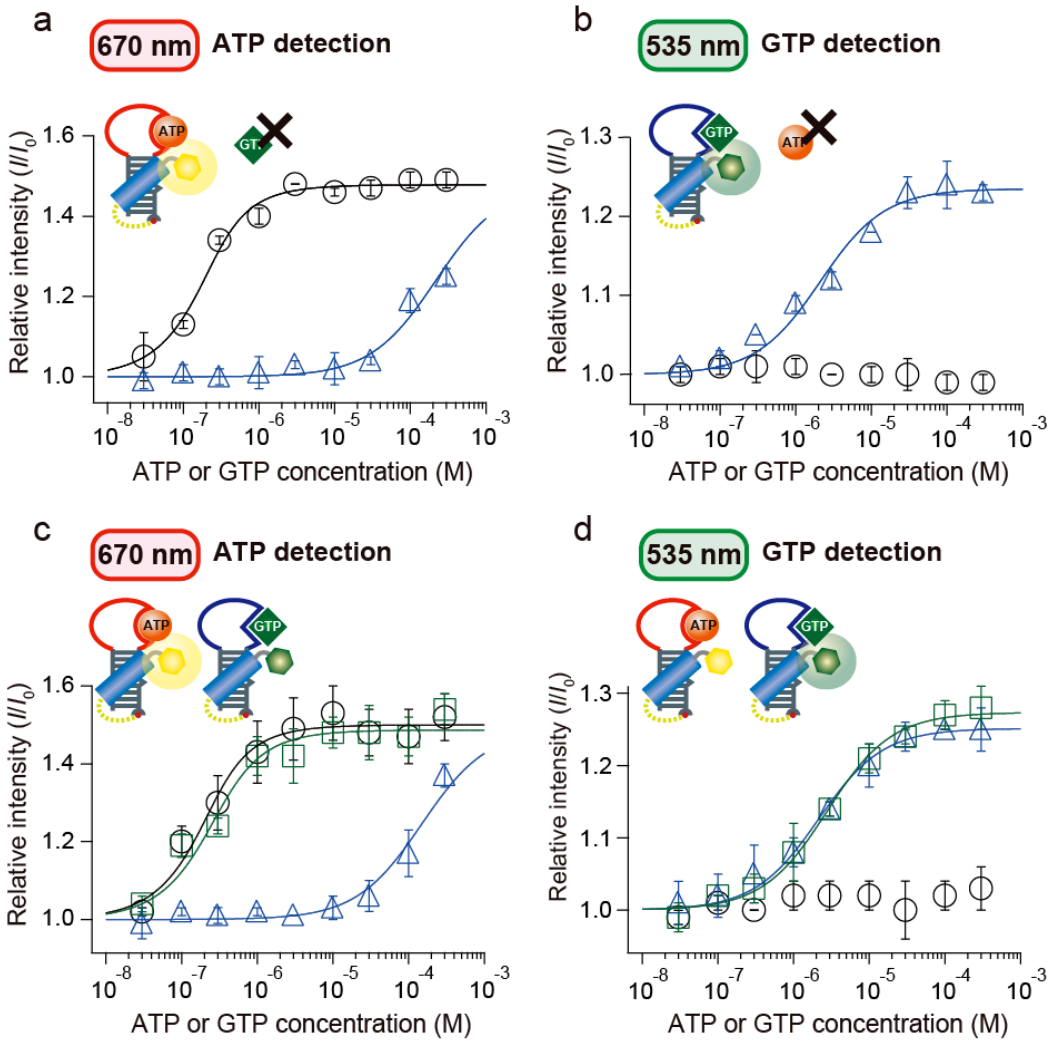

e

sensor	substrate		
	ATP	GTP	ATP+GTP
c-An16/Cy5-Rev	< 200 nM	> 300 μM	-
c-G23/5FAM-Rev	N.D.	2.0 μM	-
c-An16/Cy5-Rev and c-G23/5FAM-Rev	< 200 nM	2.0 μM	< 200 nM 2.3 μM

Figure S4. (a and b) Fluorescence titration analyses of c-An16/Cy5-Rev and c-G23/5FAM-Rev by ATP and GTP, respectively. Fluorescent titration analyses were performed for (a) the ATP sensor (200 nM c-An16/Cy5-Rev) at 670 nm and (b) the GTP sensor (200 nM c-G23/5FAM-Rev) at 535 nm with ATP (circles) or GTP (triangles) at 4 °C. (c and d) A solution containing both the ATP sensor c-An16/Cy5-Rev and the GTP sensor (200 nM c-G23/5FAM-Rev) was titrated with ATP (circles), GTP (triangles), or a 1:1 mixture of ATP and GTP (squares) at 4 °C. Detection at (c) 670 nm or at (d) 535 nm revealed a selective detection of the ATP or GTP concentration. (e) Dissociation constants of the c-RNP sensors for ATP and/or GTP in the absence or presence of the other sensor.

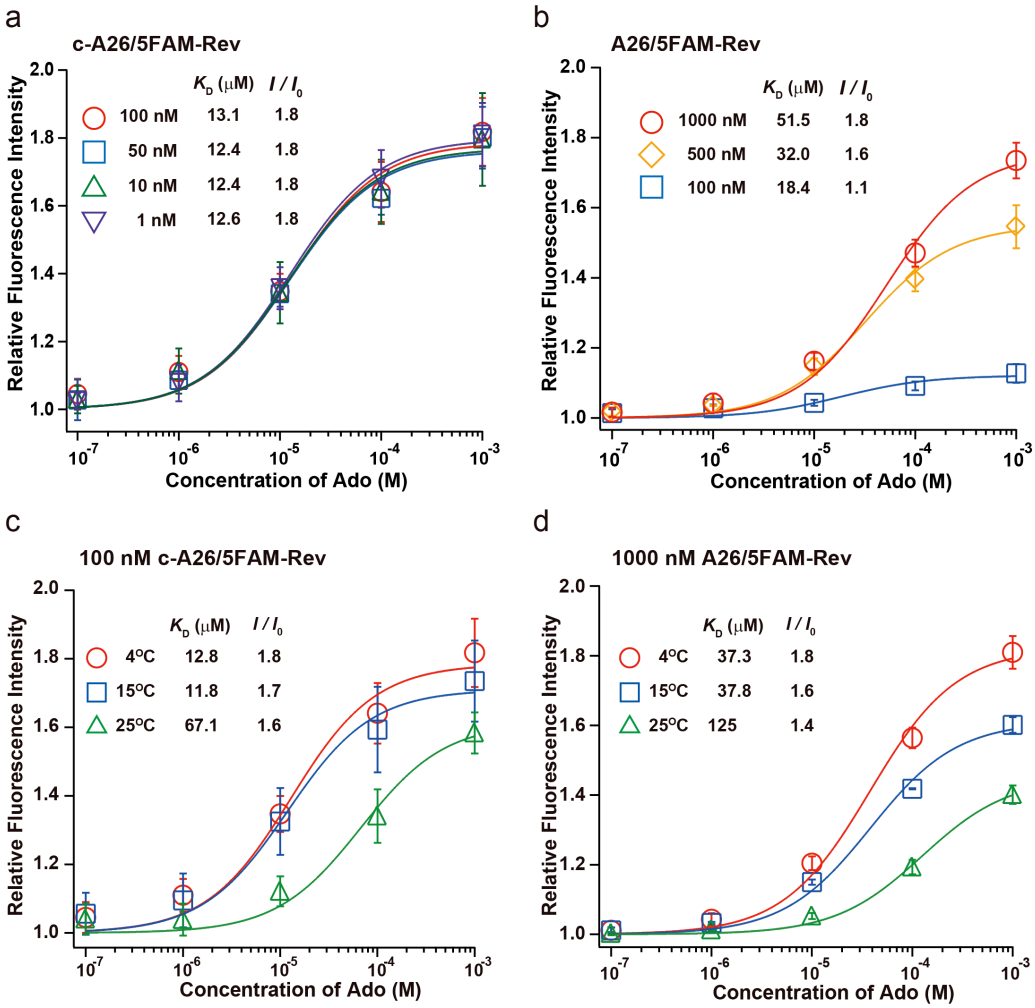

Figure S5. Saturation curves for the relative fluorescence intensity changes of c-A26/5FAM-Rev and A26/5FAM-Rev by titration with Ado in a buffer containing 10 mM Tris-HCl (pH 7.6), 100 mM NaCl, 10 mM $MgCl_2$, and 0.005% Tween 20. (a) Titration of the ATP-binding fluorescent RNP complexes c-A26/5FAM-Rev (1 nM, purple reverse triangles; 10 nM, green triangles; 100 nM, blue squares; 1000 nM, red circles) with ATP at 4°C and (b) A26/5FAM-Rev (100 nM, blue squares; 500 nM, orange diamonds; 1000 nM, red circles) with Ado at 4°C are shown. (c) Titration profiles of the ATP-binding fluorescent RNP complexes c-A26/5FAM-Rev and (d) A26/5FAM-Rev with Ado at different temperatures (4°C, red circles; 15°C, blue squares; 25°C, green triangles) are shown. The dissociation constant (K_D) and the maximum relative fluorescence intensity for the ATP complex of each RNP are shown in the inset.

a

Ado

Conc.(M)	Peak Area		AVERAGE	STDEV
5.00E−06	1583682	1594441	1589062	7607.762
1.00E−05	3168795	3113089	3140942	39390.09
3.00E−05	9210106	9654954	9432530	314555
5.00E−05	15473095	15851250	15662173	267396
1.00E−04	30645934	30928457	30787196	199773.9

b

Ino

Conc.(M)	Peak Area		AVERAGE	STDEV
5.00E−06	821139	822594	821866.5	1028.84
1.00E−05	1685342	1678197	1681770	5052.278
3.00E−05	5008189	5081906	5045048	52125.79
5.00E−05	8302298	8121027	8211663	128178
1.00E−04	15841737	16358644	16100191	365508.4

c

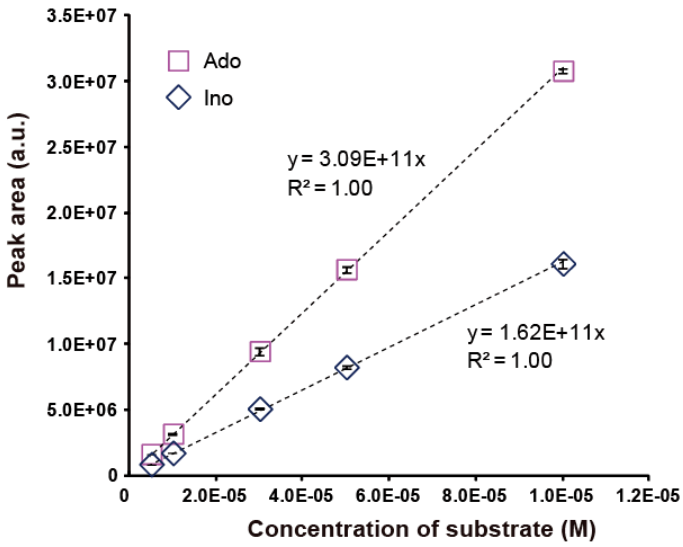

Figure S6. Quantitation of the peak area for given concentration (5, 10, 30, 50 and 100 μM) of (a) Ado and (b) Ino measured by HPLC analysis. The values were used for calculating standard curves for the quantitation of the adenosine deaminase reaction. (c) The standard curves for conversion from the peak area to the substrate concentration, Ado (pink squares) and Ino (blue diamonds).

a

Ado

Time (min.)	Peak Area		AVERAGE	STDEV	Conc.(M)	STDEV
10	28134495	28817409	28475952	482893.1	9.20E−05	1.56E−06
20	25915155	25867266	25891211	33862.64	8.37E−05	1.09E−07
30	23062558	22854242	22958400	147301.7	7.42E−05	4.76E−07
45	20979005	18025710	19502358	2088295	6.30E−05	6.75E−06
60	21460113	13490595	17475354	5635300	5.65E−05	1.82E−05
75	10540923	12677526	11609225	1510806	3.75E−05	4.88E−06
90	11804339	9490117	10647228	1636402	3.44E−05	5.29E−06
120	4325588	4712975	4519282	273924	1.46E−05	8.85E−07
150	2444097	2104671	2274384	240010.4	7.35E−06	7.76E−07

b

Ino

Time (min.)	Peak Area		AVERAGE	STDEV	Conc.(M)	STDEV
10	1653414	1372831	1513123	198402.1	9.33E−06	1.22E−06
20	3149986	2967195	3058591	129252.8	1.89E−05	7.97E−07
30	4360427	4101340	4230884	183202.2	2.61E−05	1.13E−06
45	5532600	6441466	5987033	642665.3	3.69E−05	3.96E−06
60	5301724	9125868	7213796	2704078	4.45E−05	1.67E−05
75	10622805	9761406	10192106	609101.1	6.29E−05	3.76E−06
90	10104132	11235664	10669898	800114	6.58E−05	4.93E−06
120	13735474	13647309	13691392	62342.07	8.44E−05	3.85E−07
150	14390796	15054706	14722751	469455.3	9.08E−05	2.90E−06

c

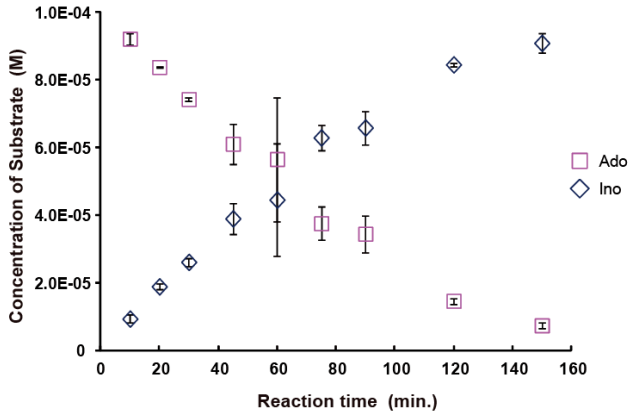

Figure S7. Peak area of (a) substrate (Ado) and (b) product (Ino) measured by HPLC analyses in the adenosine deaminase reaction at a given reaction time (10, 20, 30, 45, 60, 75, 90, 120 and 150 min.). (c) Time course profiles for the concentration changes of Ado (pink squares) and Ino (blue diamonds) in the adenosine deaminase reaction. Concentrations of Ado and Ino were converted from the peak area by using the standard curves (Figure S6). A sample was prepared by mixing c-A26/5FAM-Rev, c-G23/Pyr-Rev, and 100 μM Ado in 10 mM Tris-HCl (pH 7.6) containing 100 mM NaCl, 10 mM $MgCl_2$, and 0.005% Tween 20. The sample was incubated for 30 min at 15°C, and then 0.1 mU of ADA was added to start the reaction.

a

100 nM c-A26/5FAM-Rev

Ado Conc (M)	Fluorescence Intensity 535nm			AVERAGE	STDEV
0	550.7	540.7	670	587.1333	71.93861
1.00E−07	602.2	553.6	667.4	607.7333	57.10143
1.00E−06	625.5	632.9	685.8	648.0667	32.88683
1.00E−05	738	739.8	798.6	758.8	34.47956
1.00E−04	889.3	927.8	1055	957.3667	86.71657
1.00E−03	1045	942.2	1136	1041.067	96.95985

b

100 nM c-G23/Pyr-Rev

Ino Conc (M)	Fluorescence Intensity 380nm			AVERAGE	STDEV
0	647.7	492.7	677.4	605.9333	99.18096
1.00E−07	623.2	538.2	637	599.4667	53.50526
1.00E−06	686	580	644.3	636.7667	53.40003
1.00E−05	864.6	659.6	875.8	800	121.7189
1.00E−04	1788	1371	1846	1668.333	259.1261
1.00E−03	2839	2136	2725	2566.667	377.2987

c

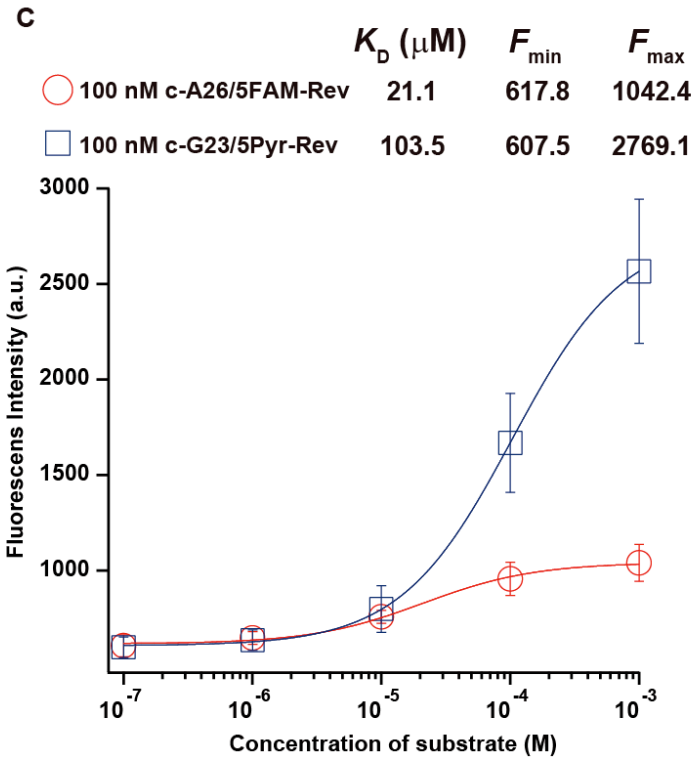

Figure S8. The ATP sensor c-A26/5FAM-Rev and the GTP sensor c-G23/Pyr-Rev were titrated with Ado at 535 nm (red circles), Ino at 380 nm (blue squares). The tables show the fluorescence intensities of c-RNP sensors (a) c-A26/5FAM-Rev with Ado and (b) c-G23/Pyr-Rev with Ino. (c) Titration curves for c-RNP sensors by Ado or Ino. Dissociation constants and the minimum and the maximum fluorescent intensity that were obtained by fitting the data to theoretical titration curves were shown above the chart.

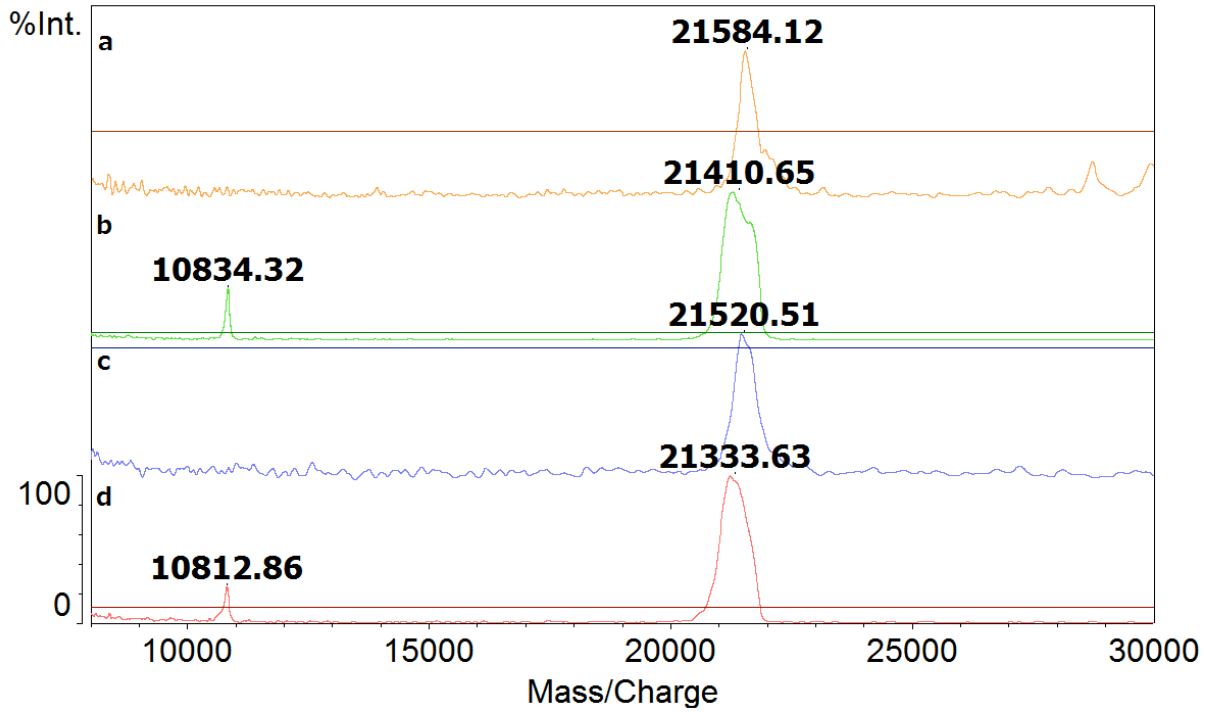

Figure S9. MALDI-TOF MS spectra of cRNP sensors. (a) c-A26/5FAM-Rev in negative mode detection (orange), (b) c-A26/5FAM in positive mode detection (light green), (c) c-G23/Pyr-Rev in negative mode detection (light purple), and (d) c-G23/Pyr-Rev in positive mode detection (pink). c-A26/5FAM-Rev: M^+ calcd: 21557.3; c-G23/Pyr-Rev: M^+ calcd: 21507.4.

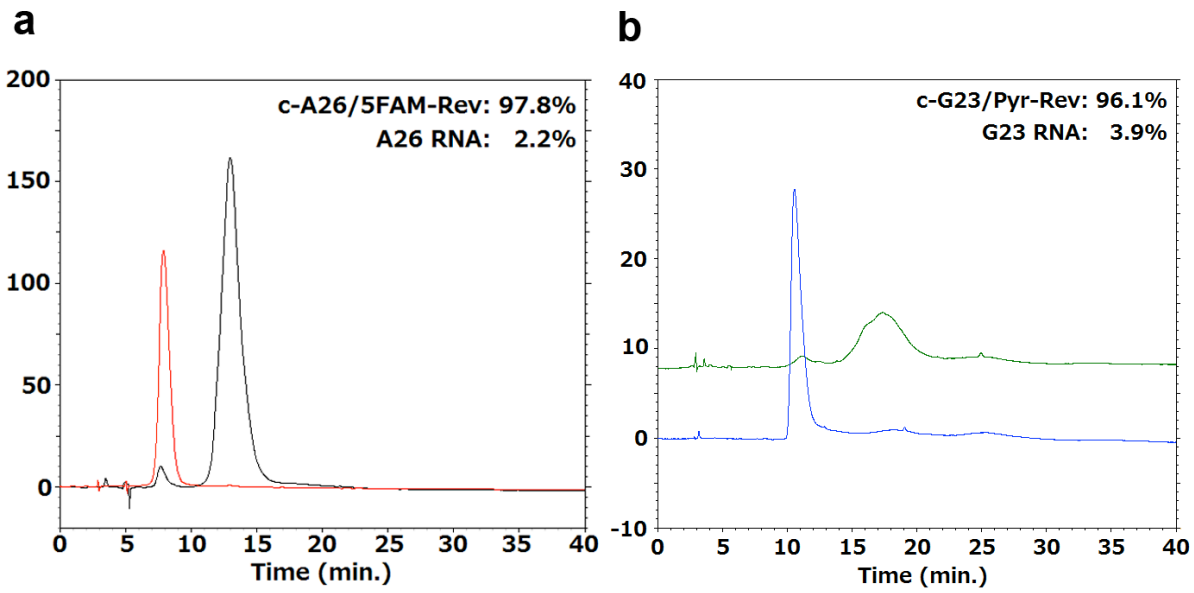

Figure S10. Reverse-phase HPLC chromatograms for the analyses of cRNP sensors c-A26/5FAM-Rev and c-G23/Pyr-Rev after purification by the denaturing gel electrophoresis (6 M Urea, 15% PAGE, Figure S2) as described in Materials and Methods. (a) A26 RNA (red line) and c-A26/5FAM-Rev after the purification (black line). (b) G23 RNA (blue line) and c-G23/Pyr-Rev after the purification (green line). The percentage for each peak area is indicated (upper right). The mobile phase consisted of 50 mM ammonium formate (eluennt A) and acetonitrile (eluent B). Samples were eluted with the gradient of eluent B increased from 3% to 23% in 40 min, and monitored at 260 nm. The flow rate was 1 mL/min for the reversed phase column Inertsil C8-3 (250 x 4.6 mm, particle size 5 µm, GL Sciences Inc).

Reference

(S1) Battiste, J. L.; Mao, H.; Rao, N. S.; Tan, R.; Muhandiram, D. R.; Kay, L. E.; Frankel, A. D.; Williamson, J. R. *Science* **1996**, *273*, 1547-1551.